Available online at www.sciencedirect.com
ScienceDirect
Journal of Sound and Vibration 306 (2007) 766–789
JOURNAL OF SOUND AND VIBRATION
www.elsevier.com/locate/jsvi

Sub-tangentially loaded and damped Beck's columns on two-parameter elastic foundation

Jun-Seok Lee[a], Nam-Il Kim[b], Moon-Young Kim[a,*]

[a]*Department of Civil and Environmental Engineering, Sungkyunkwan University, Cheoncheon-Dong, Jangan-Ku, Suwon, 440-746, South Korea*
[b]*Department of Civil and Environmental Engineering, University of Myongji, San 38-2, Nam-Dong, Yongin, Kyonggi-Do 449-728, South Korea*

Received 11 October 2006; received in revised form 13 June 2007; accepted 23 June 2007

Abstract

The dynamic stability of the damped Beck's column on two-parameter elastic foundation is investigated by using Hermitian beam elements. For this purpose, based on the extended Hamilton's principle, the dimensionless finite element (FE) formulation using the Hermitian interpolation function is presented. First, the mass matrix, the external and internal damping matrices, the elastic and the geometric stiffness matrices, Winkler and Pasternak foundation matrices, and the load correction stiffness matrix due to the sub-tangential follower force are obtained. Then, evaluation procedure for the flutter and divergence loads of the non-conservative system and the time history analysis using the Newmark-β method are shortly described. Finally, the influences of various parameters on the dynamic stability of non-conservative systems are newly addressed: (1) variation of the second flutter load due to sub-tangentiality, (2) influences of the external and the internal damping on flutter loads by analysis of complex natural frequencies, (3) the effect of the growth rate of motion in a finite time interval using time history analysis, and (4) fluctuation of divergence and flutter loads due to Winkler and Pasternak foundations.

1. Introduction

In the last 50 years, there have been many studies on the non-conservative systems under the follower force losing their stability either by divergence or by flutter. For divergence-type instability, the critical loads of the system can be determined by the static approach, whereas for flutter-type instability, the critical loads should be determined based on a dynamic criterion. A detailed discussion of this subject and a comprehensive list of references can be found in the book by Leipholz [1] and an article by Langthjem and Sugiyama [2]. In addition, it is worth referring two sharp discussions by Koiter [3] and Sugiyama et al. [4] about the nature of the follower forces.

This problem of instability is often analyzed by using numerical methods such as the finite element method [5–20]; the transfer matrix approach [21–24]; the lagrangian approach and the assumed mode method

*Corresponding author. Tel.: +82 31 290 7514; fax: +82 31 290 7548.
E-mail address: kmye@skku.ac.kr (M.-Y. Kim).

0022-460X/$ - see front matter © 2007 Elsevier Ltd. All rights reserved.
doi:10.1016/j.jsv.2007.06.017

by Lee [25–28]; the finite difference method [1,29–32] and many other forms of discretization methods [33,34].

One of the interesting topics in non-conservative stability problems has been the destabilizing effect of small damping. If such destabilization occurs, damping must be considered in the formulation of the solution, because a safe design of the system is possible only when damping is considered. Because all physical systems involve damping in one form or another, research on the stability of columns subjected to a non-conservative follower force will be very meaningful. As shown in previous works [2,35,36,10,37–47], the realistic modeling of any structure must consider and include the damping effect. Ziegler [47] first evaluated the destabilizing effect of damping by considering a viscoelastic double pendulum model. He found that the critical load for small damping could be lower than that for no damping. More information about this phenomenon for the double pendulum can be found in the works of Kounadis and Smities [38] and Kounadis [39]. Krätzig [41] found that for the Beck's column, the critical load decreases about 15% more in a damped system, with dissipation ratios of 3% with respect to the first two eigen-frequencies, than in an undamped one. Bolotin and Zhinzher [44] and Bolotin [45,46] observed the same behavior for a linear, viscoelastic column. Semler et al. [37] gave the physical explanation of the destabilizing effect of damping and discussed this effect in reference to a two-degree-of-freedom (dof) articulated system. Also, an early experimental study by Sugiyama et al. [36] on the dynamic stability of cantilevers under rocket thrust significantly clarified the destabilizing effect of small internal damping. The theoretical flutter load for the Beck's column with small internal damping is about half the flutter load for the undamped column. The destabilizing effect of damping can be described in terms of the mathematical concept of stability, and asymptotic stability in an infinite time. Here, the asymptotic stability condition implies that the dynamical system is unstable if the amplitude of the disturbed motion of the system becomes infinite as time goes to infinity. However in practice, a follower force caused by a rocket motor can act on elastic structures only for a finite time interval. Knowing this fact, Ryu and Sugiyama [5] and Sugiyama et al. [35] recently filled the gap between the analytical results obtained so far of the damping effect and the realistic aspects of the damping effect by using the finite element method. And the concept of stability in a finite time interval was applied to the study on dynamic stability of the cantilever column subjected to a follower force.

As for the problems of non-conservative stability analysis of a beam on an elastic foundation, Smith and Herrmann [48] have shown that the critical flutter load for a cantilever beam is independent of the foundation modulus for a Bernoulli–Euler beam resting on an elastic foundation. Sundararajan [49] derived a theorem that states that the critical flutter load does not decrease due to the introduction of a Winkler-type elastic foundation provided that the modulus distribution of the foundation is geometrically similar to the mass distribution of the beam. Hauger and Vetter [50] observed that a weakening of the foundation can improve the stability of the column, whereas a strengthening of it may decrease the critical load. Elishakoff and Wang [51] presented a generalization of the Smith–Herrmann problem by considering the attachment of an elastic foundation to a part of the column and Elishakoff and Jacoby [52] investigated the influence of various types of elastic foundation on the buckling and flutter loads of Ziegler's model structure. The stability of tapered cantilever columns resting on an elastic foundation subjected to a concentrated follower force at the free end was investigated by Venkateswara Rao and Kanaka Raju [53]. Lee et al. [54] and Lee and Yang [55] investigated the influences of the Winkler elastic foundation modulus and the slenderness ratio on the critical load of uniform and non-uniform Timoshenko beams, respectively, subjected to a concentrated follower force. The existing literatures related to the non-conservative stability of a beam on elastic foundation reveal no studies of the effect of internal damping, except for the study of Lee [26]. However, his study was only restricted to the analysis of a beam resting on a Winkler-type elastic foundation.

Despite these extensively cited studies for the dynamic stability analysis of the non-conservative systems, there still remain some margins to investigate the dynamic stability characteristics of columns subjected to non-conservative follower forces. In this study, finite element method (FEM) is formulated based on the extended Hamilton's principle. The effects of the sub-tangentiality of the follower forces, the external and the internal damping, and the Winkler and Pasternak foundations on the dynamic stability behavior of non-conservative systems are fully discussed. The important points presented may be summarized as follows:

1. The dimensionless FE formulation using Hermitian beam elements is employed to perform a parametric study of the damped Beck's column on two-parameter elastic supports.

2. Variation of the second flutter load due to sub-tangential follower force is newly investigated, and the corresponding stability diagram is presented by analyzing double eigen-curves.
3. Stability characteristics due to the Rayleigh damping matrix is rigorously traced by studying *complex* natural frequencies of the externally and internally damped non-conservative system.
4. The effect of growth rate of motion for a finite time interval on the Beck's column with external and internal damping is reported by using time history analysis.
5. The effects of Winkler and Pasternak foundations on the divergence and flutter loads of the damped non-conservativeness system are addressed.
6. Finally, the flutter-jump phenomena are observed depending upon the Winkler and Pasternak foundations, and the external and the internal damping.

2. FE formulation of the non-conservative system

Fig. 1 shows Beck's columns, in which the direction of the follower force sub-tangentially changes according to the rotation of the cross sections. For derivation of the equation of motion and the finite element formulation, we consider a beam-column element (Fig. 2) of length l_e with element nodal displacements (v^p, θ^p, v^q, θ^q) and element nodal forces (S^p, M^p, S^q, M^q).

In this study, the kinetic energy Π_M, the elastic strain energy Π_E of the system resting on two types of elastic foundation, the potential energy Π_G including the work done by the conservative component of the follower force, and the virtual work $\delta\Pi_{NC}$ by the non-conservative damping and follower force are considered. The extended Hamilton's principle of the column under consideration can be expressed by

$$\int_{t_1}^{t_2} [\delta(\Pi_M - \Pi_E - \Pi_G) + \delta\Pi_{NC}]\,\mathrm{d}t = 0, \tag{1}$$

where δ is variation of energy and each term of which is given as

$$\Pi_M = \sum_e \frac{1}{2}\int_0^{l_e} m\left(\frac{\partial v}{\partial t}\right)^2 \mathrm{d}x, \tag{2a}$$

$$\Pi_E = \sum_e \frac{1}{2}\int_0^{l_e} \left\{ EI\left(\frac{\partial^2 v}{\partial x^2}\right)^2 + k_1 v^2 + k_2\left(\frac{\partial v}{\partial x}\right)^2 \right\} \mathrm{d}x, \tag{2b}$$

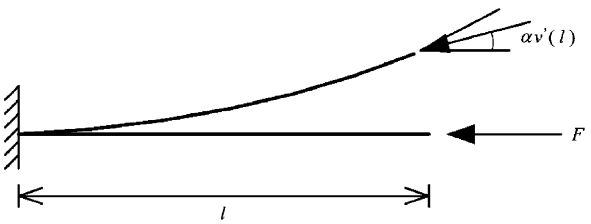

Fig. 1. Beck's column subjected to a sub-tangential follower force.

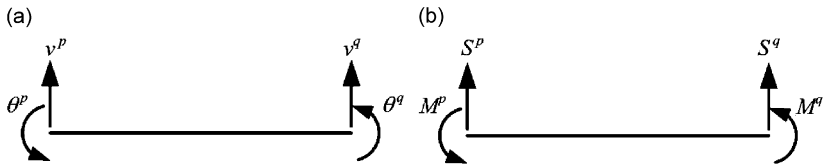

Fig. 2. Beam-column element under consideration. (a) Element nodal displacements and (b) element nodal forces.

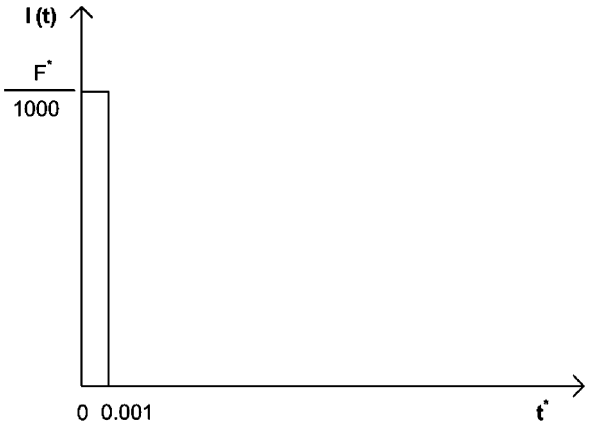

Fig. 3. Impulse loading function.

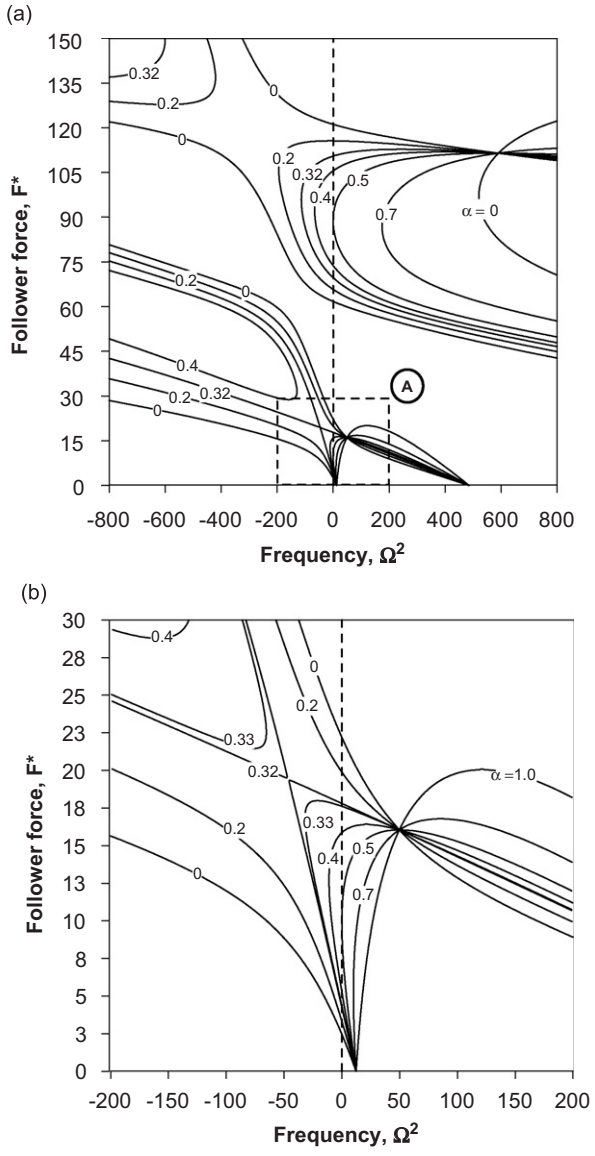

Fig. 4. Double eigen-curves including the higher divergence and flutter loads. (a) Double eigen-curves and (b) detail of Ⓐ.

$$\Pi_G = -\sum_e \frac{1}{2}\int_0^{l_e} F\left(\frac{\partial v}{\partial x}\right)^2 \mathrm{d}x, \tag{2c}$$

$$\delta\Pi_{NC} = -\sum_e \int_0^{l_e} \left\{\gamma_1 \frac{\partial v}{\partial t}\delta v + \gamma_2 \frac{\partial^3 v}{\partial t\,\partial x^2}\delta\left(\frac{\partial^2 v}{\partial x^2}\right)\right\} \mathrm{d}x - \alpha F \frac{\partial v(l)}{\partial x}\delta v(l), \tag{2d}$$

where m is the mass per unit length, EI is the flexural rigidity, k_1 and k_2 are the Winkler and Pasternak foundation parameters, respectively, and F is the follower force in the Beck's column. γ_1 and γ_2 are the external and internal damping coefficients, respectively, and α and l are the non-conservativeness parameters denoting sub-tangentiality and the total length of columns, respectively. For simplicity, the following dimensionless variables are introduced:

$$V = \frac{v}{l}, \quad x^* = \frac{x}{l}, \quad t^* = \frac{t\sqrt{EI/m}}{l^2}, \quad k_1^* = \frac{k_1 l^4}{EI}, \quad k_2^* = \frac{k_2 l^2}{EI},$$
$$F^* = \frac{Fl^2}{EI}, \quad \gamma_1^* = \frac{\gamma_1 l^2}{\sqrt{EIm}}, \quad \gamma_2^* = \frac{\gamma_2}{l^2\sqrt{EIm}}, \quad \Omega = \sqrt{\frac{ml^4}{EI}}\omega, \tag{3a–i}$$

where ω is the circular frequency.

Using dimensionless variables and taking into account Eq. (1), the extended Hamilton's principle for finite element formulation can be written as follows:

$$\delta\int_{t_1^*}^{t_2^*} \Pi_C \,\mathrm{d}t^* + \int_{t_1^*}^{t_2^*} \delta\Pi_{NC}\,\mathrm{d}t^* = 0, \tag{4}$$

where

$$\Pi_C = \frac{1}{2}\sum_e \left\{\int_0^{\zeta} \left(\frac{\partial v^*}{\partial t^*}\right)^2 - \left(\frac{\partial^2 v^*}{\partial x^{*2}}\right)^2 - k_1^* v^{*2} - k_2^*\left(\frac{\partial v^*}{\partial x^*}\right)^2 + F^*\left(\frac{\partial v^*}{\partial x^*}\right)^2 \mathrm{d}x^*\right\}, \tag{5a}$$

$$\delta\Pi_{NC} = -\sum_e \int_0^{\zeta} \left\{\gamma_1^* \frac{\partial v^*}{\partial t^*}\delta v^* + \gamma_2^* \frac{\partial^3 v^*}{\partial t^*\partial x^{*2}}\delta\left(\frac{\partial^2 v^*}{\partial x^{*2}}\right)\right\} \mathrm{d}x^* - \alpha F^* \frac{\partial v^*(l)}{\partial x^*}\delta v^*(l), \tag{5b}$$

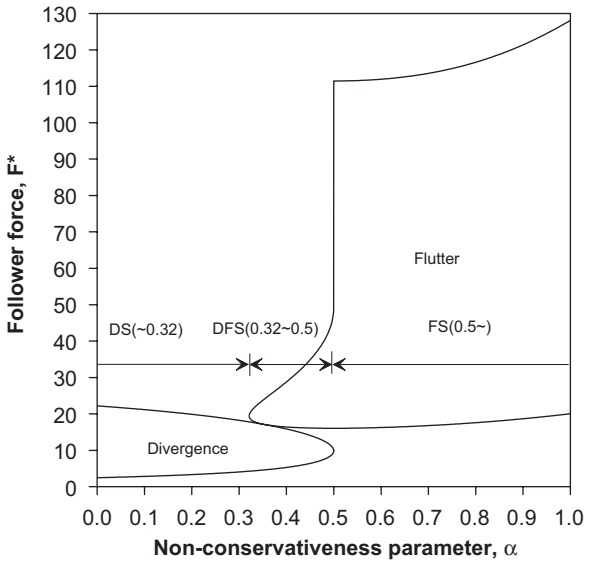

Fig. 5. Stability diagrams.

and where $\zeta(=l_e/l)$ is the dimensionless length of a beam element. As shown in Fig. 2(a), the element model presented here consists of two nodes, each of which has two dof. The vertical displacement v^* of a typical point within the element can be related to nodal displacements by using the third-order Hermitian interpolation polynomial.

Now substituting the interpolated displacement into Eq. (4), the resulting equation of motion for a single element is obtained in a matrix form as

$$\mathbf{M_e}\ddot{\mathbf{U}}_\mathbf{e} + \mathbf{C_e}\dot{\mathbf{U}}_\mathbf{e} + \left(\mathbf{K_e} + \mathbf{K_s} + \mathbf{K_g} - \mathbf{K_{nc}}\right)\mathbf{U_e} = \mathbf{F_e}, \tag{6}$$

where $\mathbf{U_e}$ and $\mathbf{F_e}$ are the nodal displacement and force vectors, respectively, $\mathbf{M_e}$ is the mass matrix, $\mathbf{C_e}$ is the damping matrix, $\mathbf{K_e}$ is the elastic stiffness matrix, $\mathbf{K_s}$ is the stiffness matrix considering the foundation effects, $\mathbf{K_g}$ is the geometric stiffness matrix due to an axial force, $\mathbf{K_{nc}}$ is the load correction stiffness matrix due to the directional change of non-conservative force. The detailed results of each matrix are presented in the

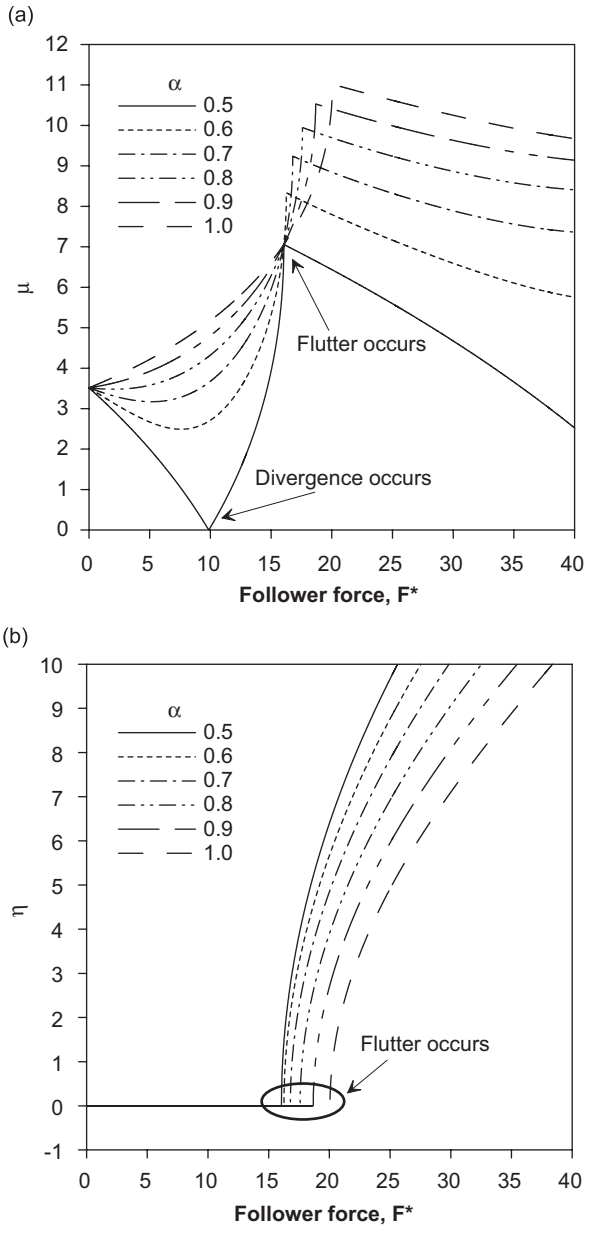

Fig. 6. Variation of the complex frequency versus the follower force with various α. (a) Variation of μ and (b) variation of η.

Table 1
The flutter loads of Beck's column

γ_1^*/γ_2^*	0	0.1	1	10	100
0	20.05 (20.05)	20.05	20.11	24.28	37.22
0.0001	10.94 (10.94)	19.91	20.11	24.29	37.22
0.001	10.94 (10.94)	17.56	19.98	24.38	37.21
0.01	10.97 (10.97)	12.93	17.80	25.20	37.21
0.1	13.64 (13.64)	14.08	17.33	32.10	37.38
0.2	21.51 (21.53)	21.98	25.86	41.31	37.85

Results in parenthesis are from Nageswara Rao and Venkateswara Rao [30].

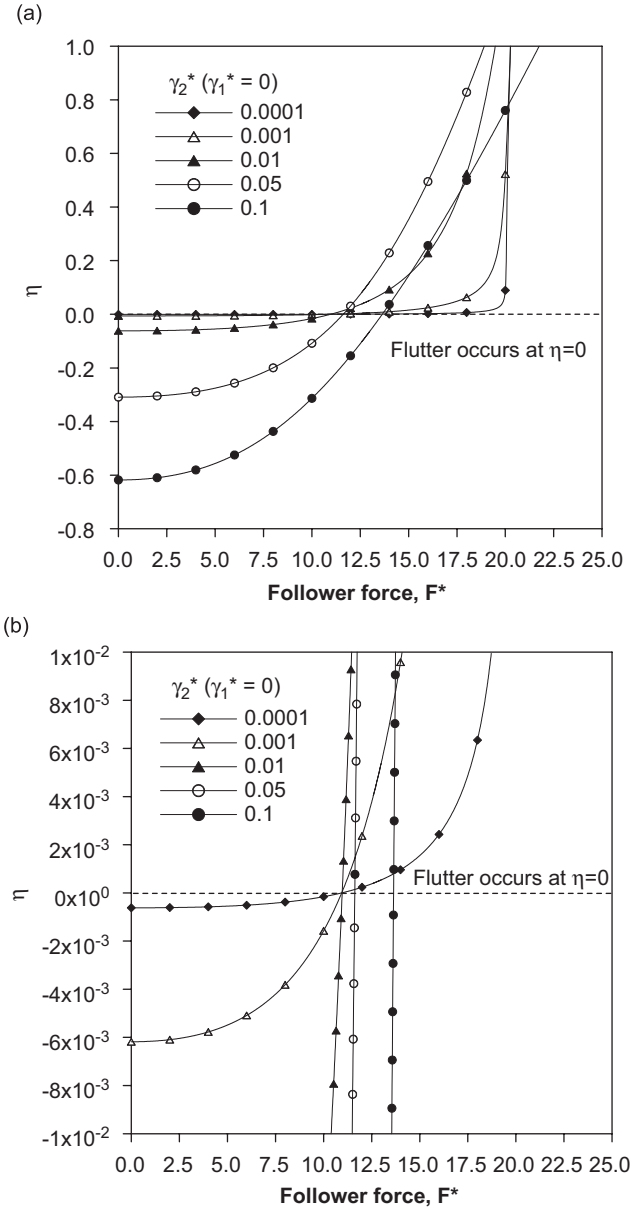

Fig. 7. Variation of η for the column with only internal damping when $\alpha = 1.0$. (a) Variation of η when $\alpha = 1.0$ and (b) detail of Fig. 7(a).

Appendix. Note that the damping matrix $\mathbf{C_e}$ due to the external and internal damping is represented by a linear combination of the mass matrix and the elastic stiffness matrix and resultantly, takes the same form as the Rayleigh damping matrix [60] as follows:

$$\mathbf{C_e} = \frac{\gamma_1^*\zeta}{420}\begin{bmatrix} 156 & 22\zeta & 54 & -13\zeta \\ & 4\zeta^2 & 13\zeta & -3\zeta^2 \\ & & 156 & -22\zeta \\ & \text{symm.} & & 4\zeta^2 \end{bmatrix} + \frac{\gamma_2^*}{\zeta^3}\begin{bmatrix} 12 & 6\zeta & -12 & 6\zeta \\ & 4\zeta^2 & -6\zeta & 2\zeta^2 \\ & & 12 & -6\zeta \\ & \text{symm.} & & 4\zeta^2 \end{bmatrix} = \gamma_1^*\mathbf{M_e} + \gamma_2^*\mathbf{K_e}. \tag{7}$$

Now using the direct stiffness method, we can obtain the equation of motion for the whole column in matrix form:

$$\mathbf{M_E}\ddot{\mathbf{U}} + \mathbf{C_E}\dot{\mathbf{U}} + (\mathbf{K_E} + \mathbf{K_S} + \mathbf{K_G} - \mathbf{K_{NC}})\mathbf{U} = \mathbf{F}, \tag{8}$$

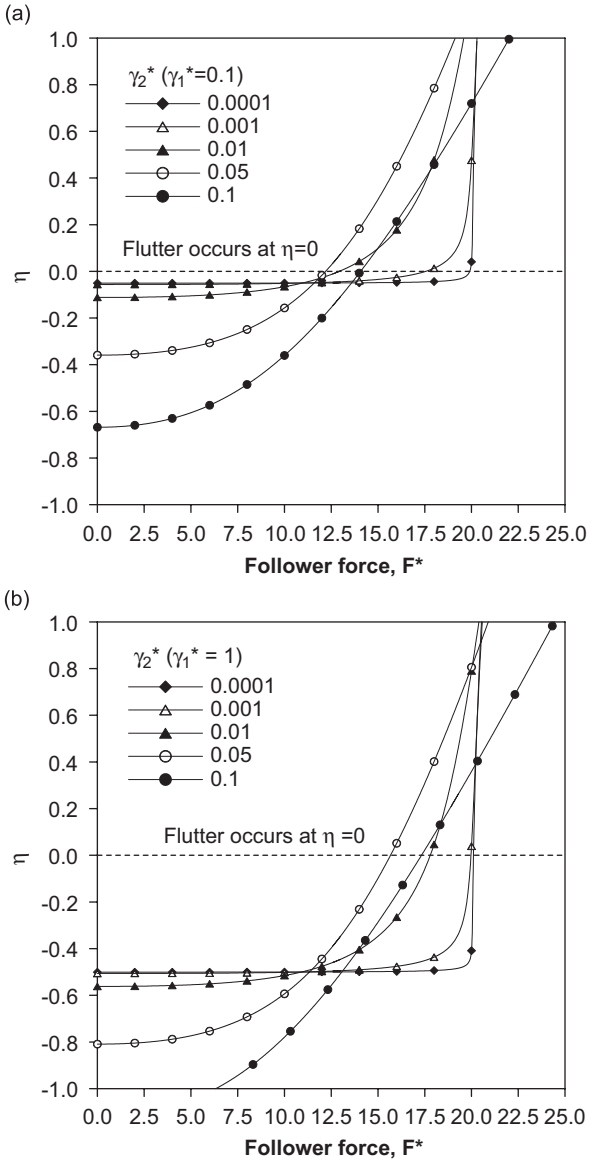

Fig. 8. Variation of η for the column with external and internal damping. (a) $\alpha = 1.0$ and $\gamma_1^* = 0.1$ and (b) $\alpha = 1.0$ and $\gamma_1^* = 1.0$.

where $\mathbf{M_E}$, $\mathbf{C_E}$,$\mathbf{K_E}$ and $\mathbf{K_G}$ are, respectively, the mass-, the damping-, the elastic stiffness-, the geometric stiffness matrices in the global coordinate system. $\mathbf{K_s}$ and $\mathbf{K_{NC}}$ are the global stiffness matrices considering the foundation effects and the load correction stiffness matrix due to circulatory forces, respectively.

3. Dynamic stability analysis

In this section, the method evaluating the critical loads of a non-conservative system and the time history analysis for impulse loads are shortly described. The global stiffness matrix of a system is asymmetric due to the effect of non-conservative forces, so that the IMSL [56] subroutine, which can provide the complex eigenvalue of asymmetric matrix equation, is used.

3.1. Divergence and flutter systems without damping

If only the unstable static equilibrium state of a non-conservative system without damping is considered, the terms corresponding to the mass matrix $\mathbf{M_E}$, the damping matrix $\mathbf{C_E}$, and the force vector $\mathbf{F}$ vanish. Consequently, the following eigenvalue problem from Eq. (8) can be considered:

$$(\mathbf{K_E} + \mathbf{K_S})\mathbf{U} = \lambda(\mathbf{K_G} - \mathbf{K_{NC}})\mathbf{U}, \tag{9}$$

where λ is the proportionality parameter. The critical divergence load F_d^* of the system is determined by calculating the eigenvalue λ of Eq. (9).i.e., by performing the conventional buckling analysis, although the system matrix is non-symmetric. Also, for the undamped flutter system, Eq. (8) is simplified to

$$\mathbf{M_E}\ddot{\mathbf{U}} + [\mathbf{K_E} + \mathbf{K_S} - \lambda(\mathbf{K_G} - \mathbf{K_{NC}})]\mathbf{U} = 0. \tag{10}$$

By setting $\mathbf{U} = e^{i\Omega t*}\mathbf{H}$, Eq. (10) is reduced to the double eigenvalue problem as

$$[\mathbf{K_E} + \mathbf{K_S} - \lambda(\mathbf{K_G} - \mathbf{K_{NC}})]\mathbf{H} = \Omega^2\mathbf{M_E}\mathbf{H}. \tag{11}$$

The dynamic stability behaviors of an undamped non-conservative system may be traced by constructing the double eigen-curve, which shows variation of frequencies Ω^2 with the increase of the follower force λ. That is, Ω^2 becomes the positive real when λ is small. But as λ increases gradually, the first and the second frequencies approach each other, and stability is lost when two consecutive eigenvalues of Ω^2 become equal at a finite

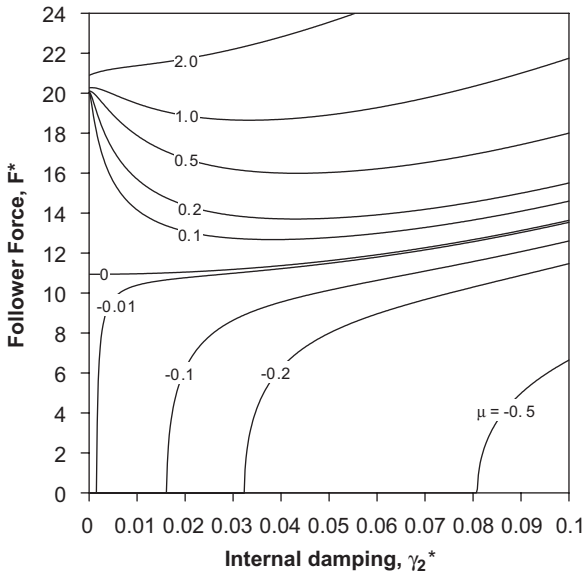

Fig. 9. Variation of the follower forces versus the internal damping with the constant μ.

critical value of λ. Beyond this value known as the flutter load F_{fl}^{*}, the perturbed motion of the system displays the diverging oscillations with increasing amplitudes while the critical eigenvalues become complex conjugates. In this study, the second flutter load as well as the first flutter load is evaluated from the double eigen-curve of Beck's column.

3.2. Flutter system with damping

For the damped flutter system, as **F** vanishes, Eq. (8) can be written as

$$\mathbf{M_E}\ddot{\mathbf{U}} + \mathbf{C_E}\dot{\mathbf{U}} + [\mathbf{K_E} + \mathbf{K_S} - \lambda(\mathbf{K_G} - \mathbf{K_{NC}})]\mathbf{U} = 0. \tag{12}$$

By setting the nodal velocity vector ($\dot{\mathbf{U}} = \mathbf{V}$) as the independent variable, Eq. (12) is transformed into two simultaneous differential equations of the first order:

$$\mathbf{M_E}\dot{\mathbf{U}} = \mathbf{M_E}\mathbf{V}, \tag{13a}$$

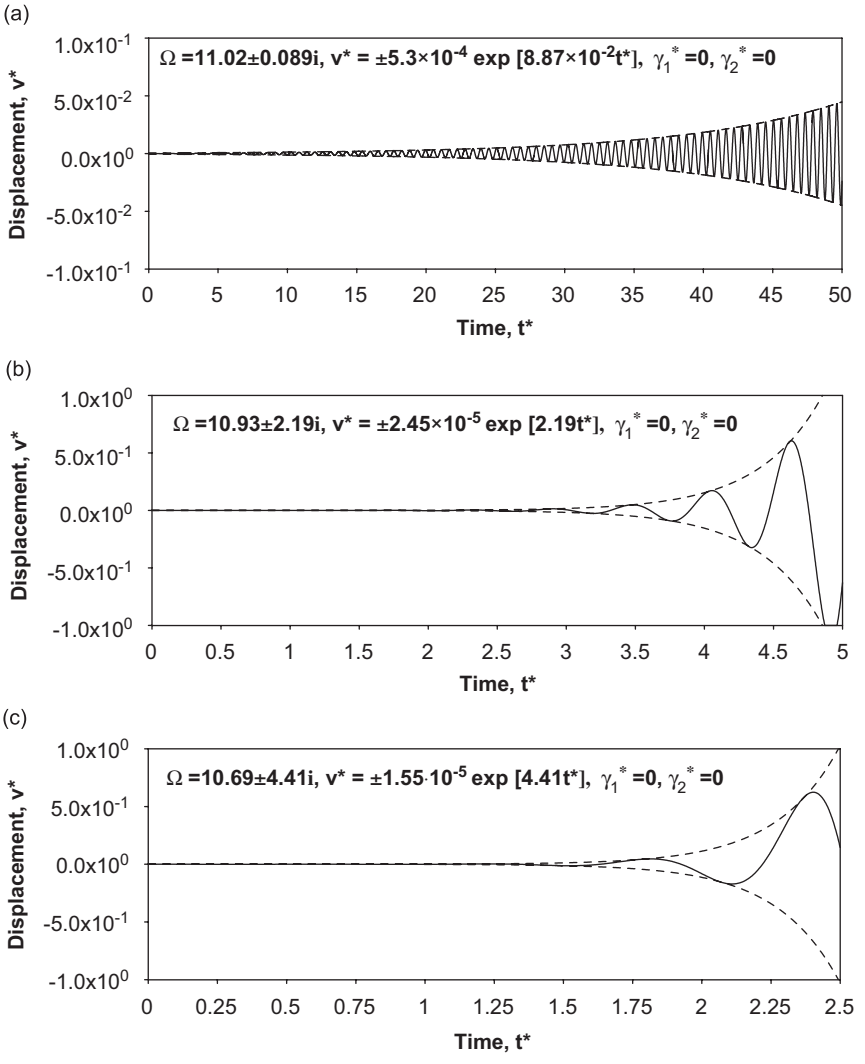

Fig. 10. Response of the column without damping. (a) $* = F_{f1}^{*} = 20.054$, (b) $* = 1.05F_{f1}^{*} = 21.057$ and (c) $* = 1.2F_{f1}^{*} = 24.065$.

$$\mathbf{M_E}\dot{\mathbf{V}} = -\mathbf{C_E}\mathbf{V} - [\mathbf{K_E} + \mathbf{K_S} - \lambda(\mathbf{K_G} - \mathbf{K_{NC}})]\mathbf{U}. \tag{13b}$$

Eq. (13) can be next expressed as an eigenvalue problem by putting $\mathbf{U} = e^{i\Omega t*}\mathbf{Q}$ and $\mathbf{V} = e^{i\Omega t*}\mathbf{S}$.

$$i\Omega\mathbf{AD} = \mathbf{BD}, \tag{14}$$

where

$$\mathbf{A} = \begin{bmatrix} \mathbf{M_E} & 0 \\ 0 & \mathbf{M_E} \end{bmatrix}, \quad \mathbf{B} = \begin{bmatrix} 0 & \mathbf{M_E} \\ -\mathbf{K_E} - \mathbf{K_S} + \lambda(\mathbf{K_G} - \mathbf{K_{NC}}) & -\mathbf{C_E} \end{bmatrix}, \quad \mathbf{D} = \{\mathbf{Q}, \mathbf{S}\}^T \tag{15a–c}$$

In case of the damped non-conservative system with small values of λ, the frequency $\Omega(=\mu \pm \eta i)$ becomes a complex conjugate, in which μ is negative. As λ increases gradually, μ approaches zero. Finally, instability occurs when μ changes from negative to positive at a finite value of λ. This value is called the flutter load F_{fl}^* of the damped system.

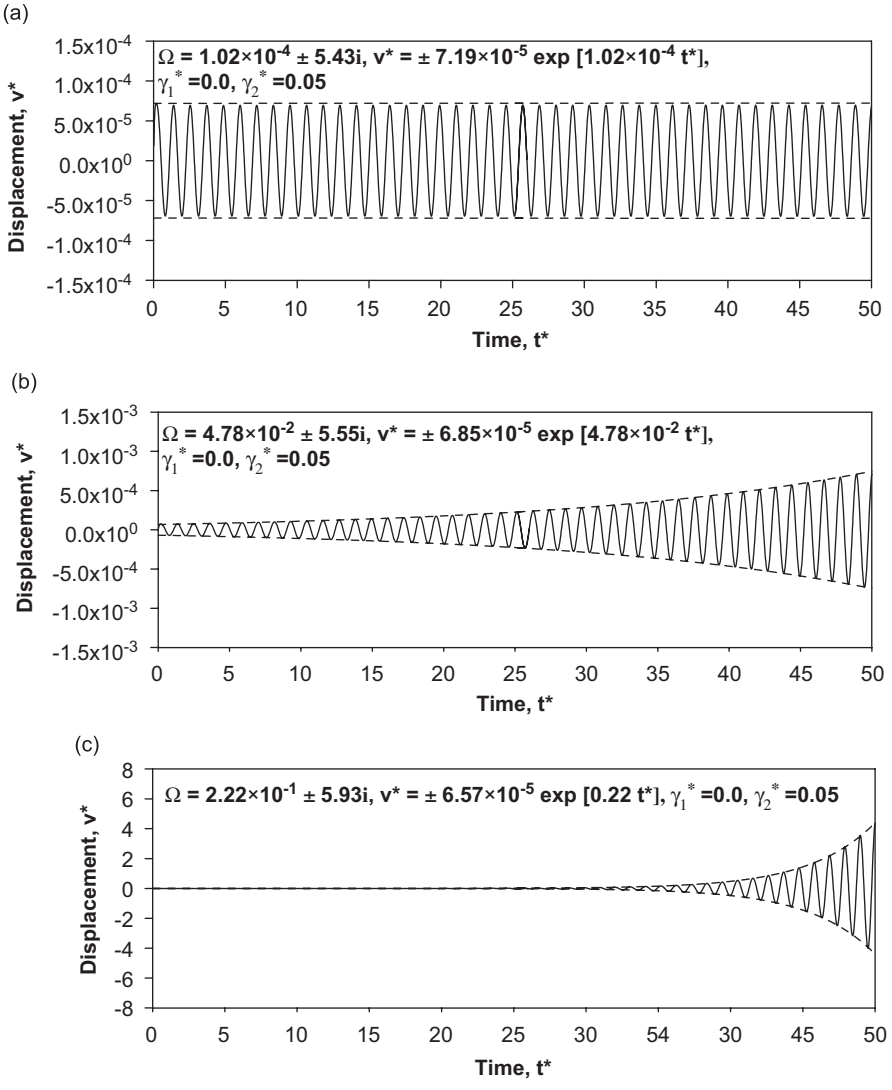

Fig. 11. Response of the column with internal damping. (a) $* = F_{f1}^* = 11.62$, (b) $* = 1.05F_{f1}^* = 12.20$ and (c) $* = 1.2F_{f1}^* = 13.94$.

3.3. Time history analysis of the non-conservative system using Newmark-β method

Instability of the non-conservative system may be investigated via the time history analysis of the perturbed system subjected to an impulse loading using the Newmark-β method. For this, the equation of motion accounting for the impulse loading is considered as follows:

$$\mathbf{M_E}\ddot{\mathbf{U}} + \mathbf{C_E}\dot{\mathbf{U}} + [\mathbf{K_E} + \mathbf{K_S} - \lambda(\mathbf{K_G} - \mathbf{K_{NC}})]\mathbf{U} = \mathbf{I}(t), \tag{16}$$

where $\mathbf{I}(t)$ denotes the impulse loading having its magnitude of $0.001F^*$ acting at the end of cantilever during only the time interval of 0.001 in the dimensionless time domain t^* (see Fig. 3).

4. Numerical examples

A parametric study is performed by using the FE analysis. Here, the Beck's column is modeled by using 10 Hermitian beam elements.

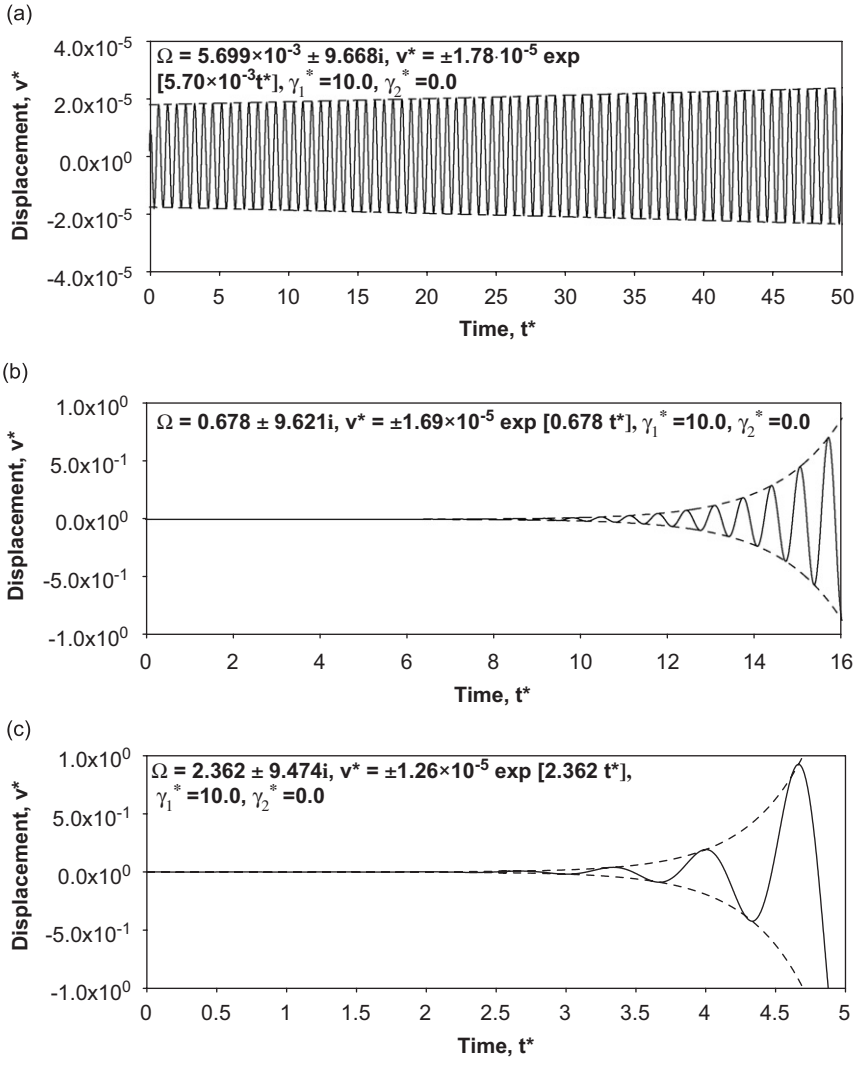

Fig. 12. Response of the column with external damping. (a) $* = F^*_{f1} = 24.28$, (b) $* = 1.05F^*_{f1} = 25.49$ and (c) $* = 1.2F^*_{f1} = 29.14$.

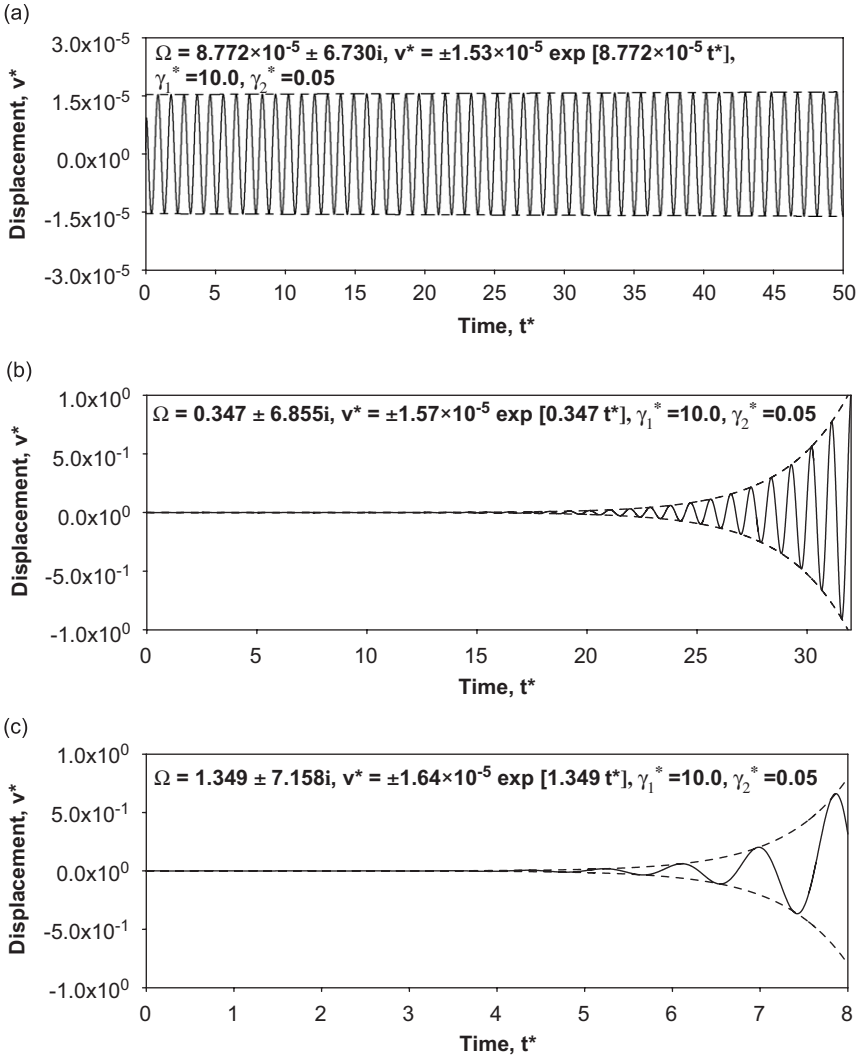

Fig. 13. Response of the column with external and internal damping. (a) $* = F^*_{f1} = 28.15$, (b) $* = 1.05F^*_{f1} = 29.56$ and (c) $* = 1.2F^*_{f1} = 33.78$.

Table 2
Dimensionless natural frequencies of beam on Winkler foundation subjected to an axial force

Mode	This study	Lee et al. [57]	Yokoyama [58]
1	9.87	9.87	9.87
2	37.19	37.19	37.20
3	86.16	86.15	86.27

4.1. Effect of non-conservativeness parameter: sub-tangentiality

In the first parametric study, the influence of the non-conservativeness parameter α on the divergence and flutter instabilities of the column is investigated. The instability of the Beck's column force changing from a constant direction ($\alpha = 0$) to a purely tangential one ($\alpha = 1$), is taken into consideration.

Fig. 4 shows the double eigen-curves of the Beck's column for the follower force versus the 1st through the 4th frequencies for various values of α. As shown in Fig. 4(b), when $0.0 \leqslant \alpha < 0.32$, the first instability

mechanism of the system is the divergence system (DS) and the first and second flutter occur with divergence at $0.32 \leqslant \alpha < 0.5$, which corresponds to the divergence-flutter system (DFS). And the pure flutter without divergence, which means the flutter system (FS), occurs at $\alpha \geqslant 0.5$.

Next, the stability diagram for the Beck's column, which shows the variation of the divergence and flutter loads with increase of α, are plotted in Fig. 5. Fig. 4 shows that not only the first flutter but also the second flutter occurs at the load level, in which the first and second frequencies coincide in DFS, while the second flutter occurs when the third and fourth frequencies become equal in FS. Due to this reason, the second flutter load in Fig. 5 is discontinuous at $\alpha = 0.5$, which corresponds to the transition point from DFS to FS. Moreover, the first and second flutter loads increase with the increase of α, as shown in Fig. 5.

In Fig. 6, the real value μ and the imaginary one η of the frequency Ω versus the follower force for various values of α are depicted. Fig. 6(a) shows that when $\alpha = 0.5$, as the follower force increases, the value of μ decreases to zero, at which buckling occurs and increases up to the occurrence of the first flutter ($F_1^* = 16.053$). Also, Fig. 6(b) shows that the imaginary value is zero before the occurrence of flutter and increases suddenly after that. Furthermore, Fig. 6 reconfirms the phenomenon in Fig. 5, in which the flutter load increases with the increase of α.

4.2. Effect of external and internal (Rayleigh) damping parameters

The second parametric study deals with the effects of the external and the internal damping on the Beck's column with $\alpha = 1.0$. Additionally, the concept of dynamic stability in a finite time interval presented by Ru and Sugiyama [5] and Sugiyama et al. [35] is applied to the time history analysis.

Under the assumption of Rayleigh damping, the following relation between γ_1^*, γ_2^* and the proportional damping parameter ξ_i (i = mode number) may be obtained from modal decomposition:

$$\gamma_1^* - \gamma_2^* \Omega_i^2 = 2\mathrm{i}\Omega_i \xi_i, \quad i = 1, 2, \tag{17}$$

where Ω_1 and Ω_2 are the first and second natural frequencies of the cantilever beam, respectively. Two damping parameters are obtained by solving Eq. (17):

$$\begin{Bmatrix} \gamma_1^* \\ \gamma_2^* \end{Bmatrix} = \frac{2}{\Omega_1^2 - \Omega_2^2} \begin{Bmatrix} -\Omega_1 \Omega_2 (\Omega_2 \xi_1 - \Omega_1 \xi_2)\mathrm{i} \\ (\Omega_2 \xi_2 - \Omega_1 \xi_1)\mathrm{i} \end{Bmatrix}. \tag{18}$$

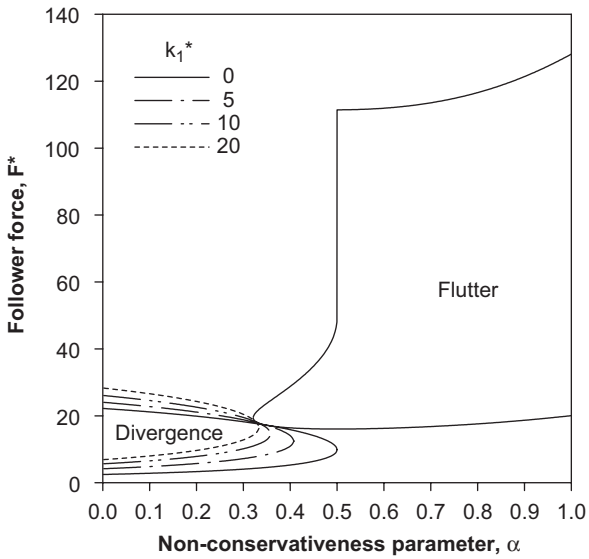

Fig. 14. Stability diagrams for the column with Winkler foundation.

Now the practical ranges of γ_1^* and γ_2^* values may be approximately determined from Eq. (18) if the suitable ranges of ξ_i are given.

In Table 1, the flutter loads F_{fl}^* for the Beck's column with various external and internal damping parameters are presented and compared with the results by Nageswara Rao and Venkateswara Rao [30] based on the finite difference method. Table 1 shows that the results of this study are in an excellent agreement with those by Ref. [30]. Also, the flutter loads for the Beck's column with very small internal damping are dramatically dropped to about half of those for the undamped columns. Then the flutter loads under no external damping increase with the increase of internal damping. In the case with small external damping ($\gamma_1^* = 0.1$ and 1), the flutter loads smoothly decrease to the critical value and then increase with the increase of

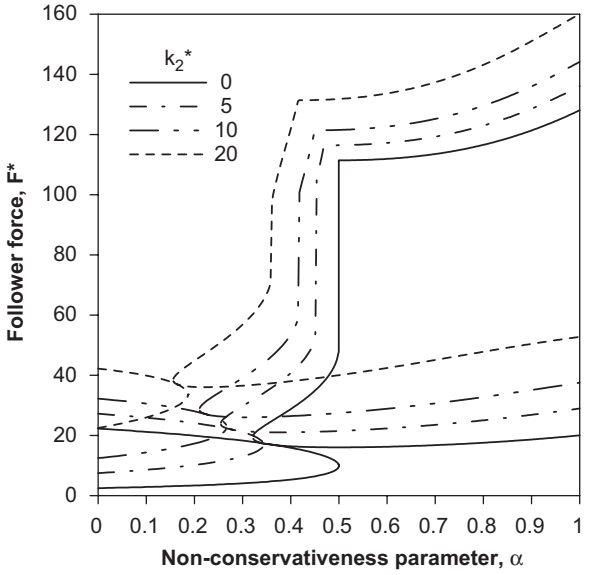

Fig. 15. Stability diagrams for the column with Pasternak foundation.

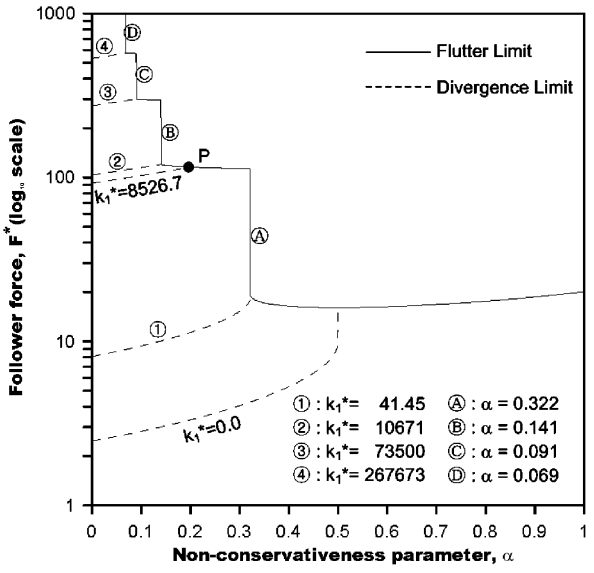

Fig. 16. Divergence and flutter instability regions for column subjected to the partially tangential force with various Winkler foundation parameters.

internal damping. Also, the flutter loads increase as the external damping increases for all values of internal damping. Fluctuation of the imaginary value η of the frequency with respect to the follower force F^* is plotted to further investigate the effects of damping on flutter loads for a damped Beck's column. Figs. 7, 8(a) and (b) show the variation of value η with respect to the follower force F^* for various internal and external dampings of $\gamma_1^* = 0.0,\ 0.1,\ 1.0$, respectively, when $\alpha = 1.0$. Note that the flutter occurs at the zero value of η. As can be seen in Fig. 7(b), the gradient of η increases as the internal damping increases; therefore, the system with a small internal damping is weakly unstable. From Figs. 8(a) and (b), it is observed that the curve is shifted down as the external damping increases. In addition, Fig. 9 shows the variation of the follower forces versus the internal damping of the column with the constant μ for $\alpha = 1.0$.

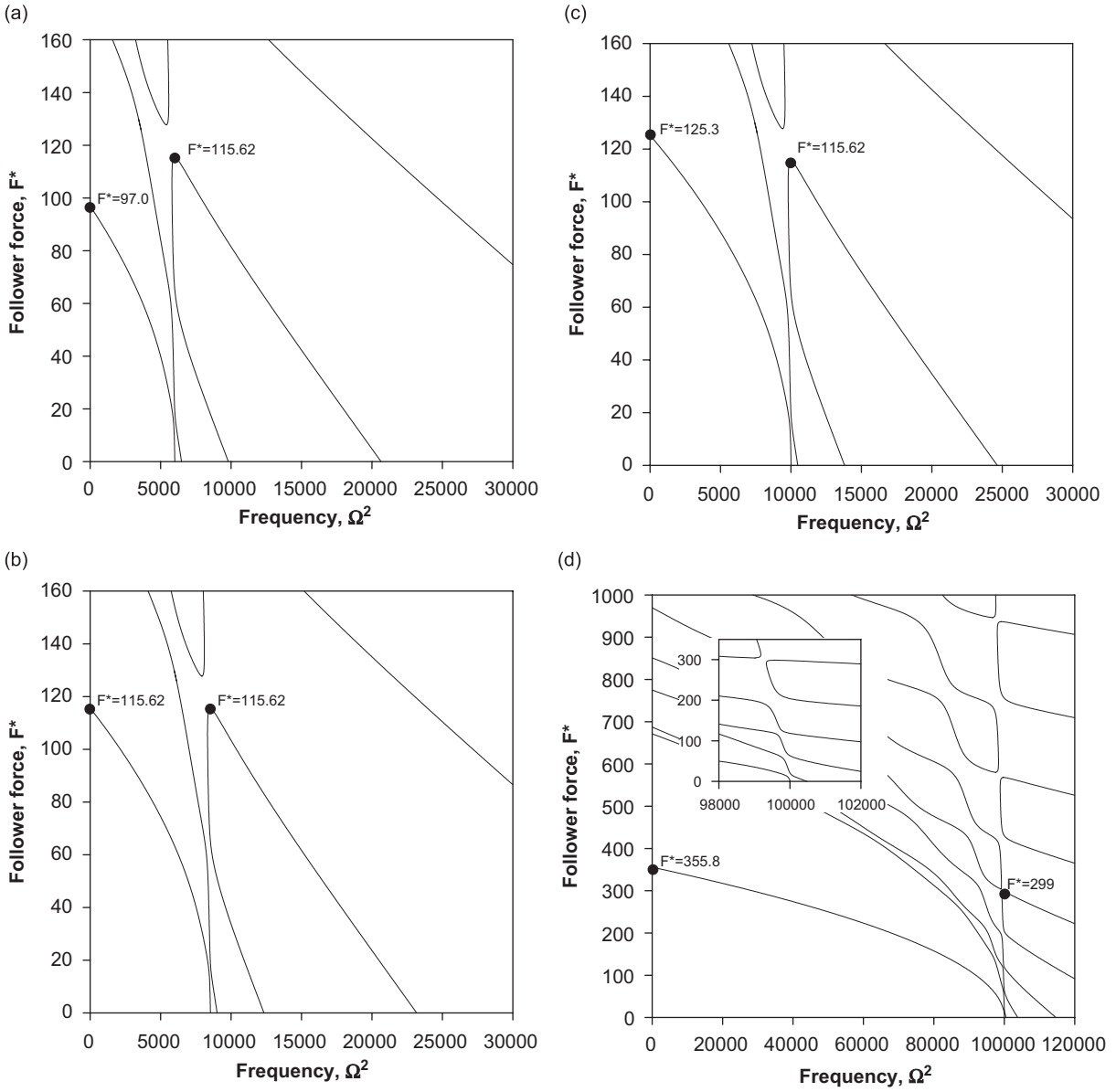

Fig. 17. Eigen-curves for the column without damping. (a) Divergence type: $\alpha = 0.2$, $k_1^* = 6000$, (b) turning point: $\alpha = 0.2$, $k_1^* = 8526.7$, (c) flutter type: $\alpha = 0.2$, $k_1^* = 10^4$ and (d) flutter type: $\alpha = 0.1$, $k_1^* = 10^5$.

To trace directly the stability behaviors of the non-conservative system, dynamic analysis is carried out by using the Newmark method. The dynamic responses of the damped Beck's column subjected to follower forces of F^*_{f1}, $1.05F^*_{f1}$ and $1.2F^*_{f1}$ are presented in Figs. 10 through 13, respectively, where the responses are those of the tip ends of the columns. The horizontal axis is the dimensionless time t^*, and the vertical axis is the dimensionless deflection v^*. The horizontal axis t^* is kept for $0 \leqslant t^* \leqslant 50$, which may be long enough to observe the growth of the motion of the column. Here, the imaginary value η of the complex eigenvalue Ω for a specified value of the follower force F^* can be referred to as the growth rate index of the motion.

Fig. 10(b) shows that the column ($\eta = 2.19$) under the follower force of $1.05F^*_{f1}$ is clearly unstable for no damping. On the other hand, Fig. 11(a) shows the steady-state motion for $\mu \approx 0$ at $F^*_{f1} = 11.62$ for the column with $\gamma^*_1 = 0.0$ and $\gamma^*_2 = 0.05$. Fig. 11(b) shows the response when $F^* = 1.05F^*_{f1}$. This response ($\mu = 0.0478$) is defined as an unstable motion in the sense of asymptotic stability where the system is considered in the infinite time interval. The small value of μ times an infinite time t^* can make a finite growth rate to indicate that the

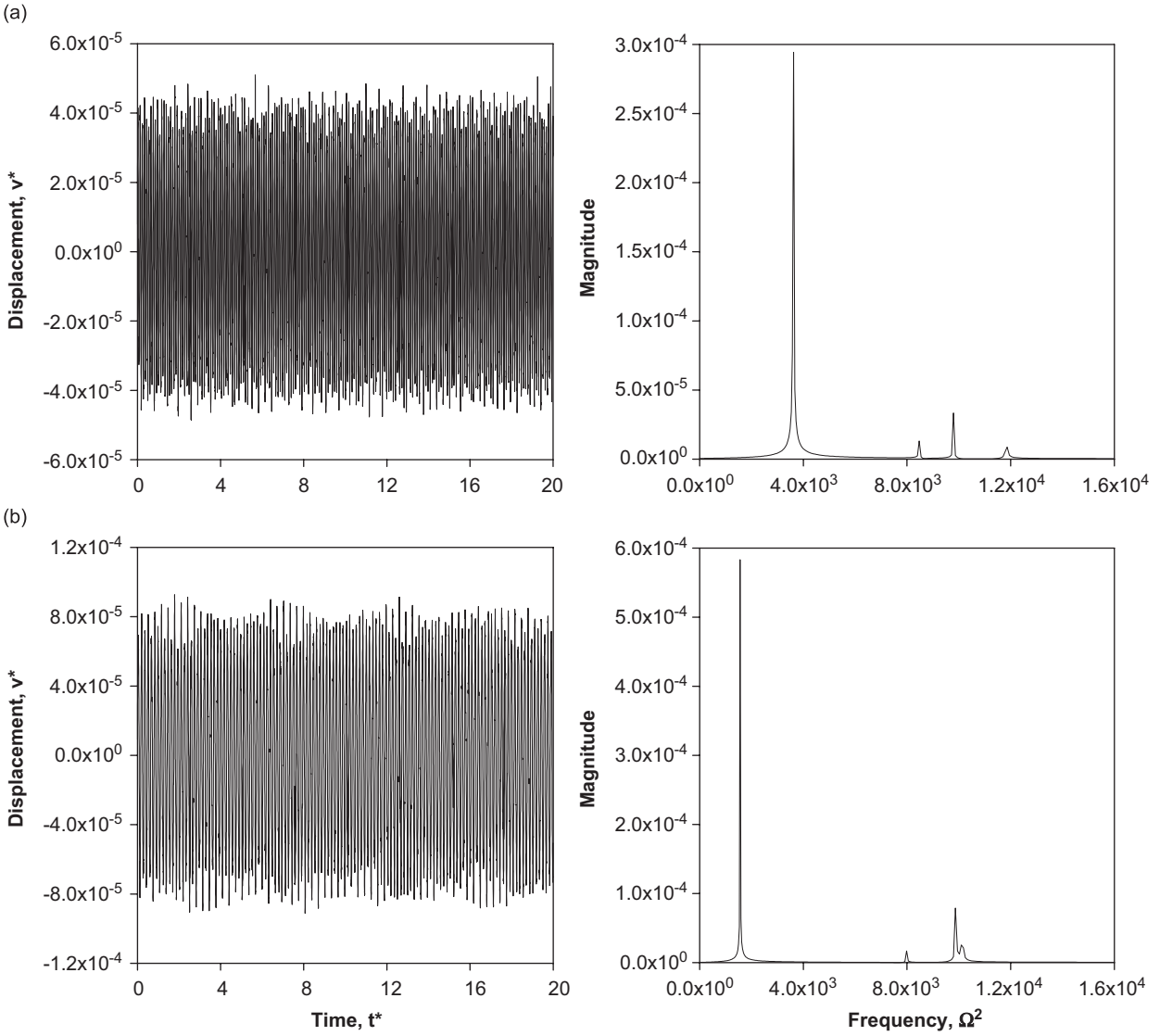

Fig. 18. Tip displacement of Beck's column as function of time and its frequency spectrum at point P (Fig. 16) when $\alpha = 0.2$, $k^*_1 = 10^4$. (a) $F^* = 100.0$, (b) $F^* = 115.0$, (c) $F^* = 115.62$ (Critical Point) and (d) $F^* = 116.0$.

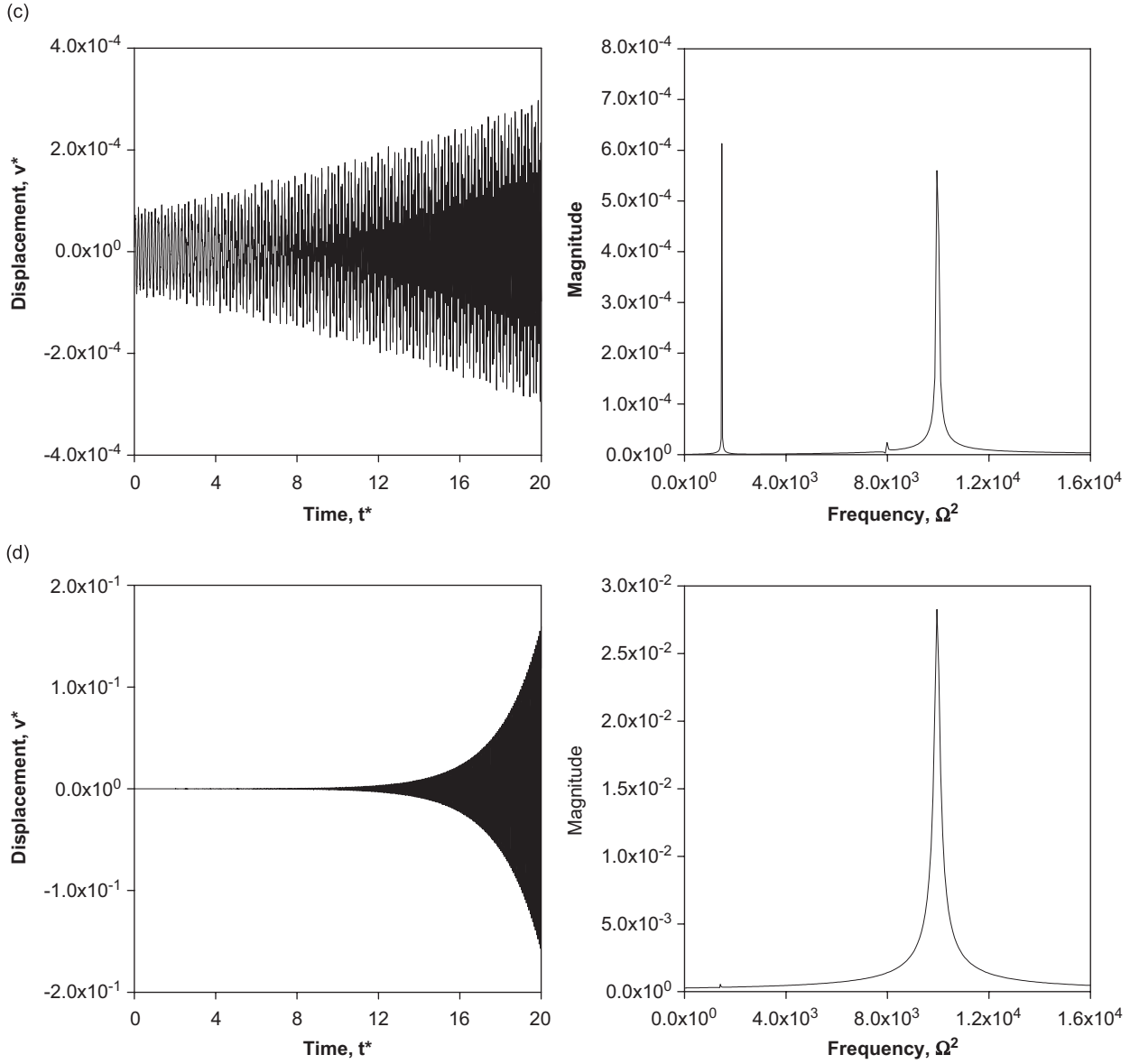

Fig. 18. (*Continued*)

system is unstable. However, in the physical aspect of stability in a finite time interval, the response shown in Fig. 11(b) can be judged as a stable motion since the dimensionless deflection v^* is very small. Also, it can be observed from Fig. 11(c) that the response of the system is a realistic unstable condition with time t^* (the maximum $v^* = 4.39$) for a large value of the follower force. In addition, Figs. 12 and 13 show the dynamic motion for the column with $\gamma_1^* = 10.0$, $\gamma_2^* = 0.0$ and $\gamma_1^* = 10.0$, $\gamma_2^* = 0.05$, respectively. Figs. 12(b) and 13(b) corresponding to $\mu = 0.678$ and 0.347, respectively, display weakly unstable behaviors.

4.3. Effect of two foundation parameters

In our final parametric study, the influence of the Winkler and Pasternak foundations on the non-conservative system is investigated. First, to verify the validity of the present element on an elastic foundation,

the first three dimensionless natural frequencies of the beam, which is under the hinge-roller boundary condition, for the foundation parameter $k_1^* = 58.445$ and subjected to an axial force $F^* = 0.6$, are presented in Table 2. For comparison, the solutions by Lee et al. [54] using the dynamic quadrature method and the results by Yokoyama [56] using the finite element technique based on the Hermitian interpolation polynomial are presented. Table 2 shows that the solutions by this study are in a good agreement with the available results.

Figs. 14 and 15 show the stability diagrams of the Beck's column for various values of Winkler and Pasternak foundation parameters, respectively, without damping. Researchers [48,49] have shown that the critical flutter load of a column is independent of the Winkler foundation parameter, as can bee seen in Fig. 14. On the other hand, Fig. 15 shows that the Pasternak-type of foundation increases the flutter as well as the divergence loads since this foundation increases the flexural stiffness of the system.

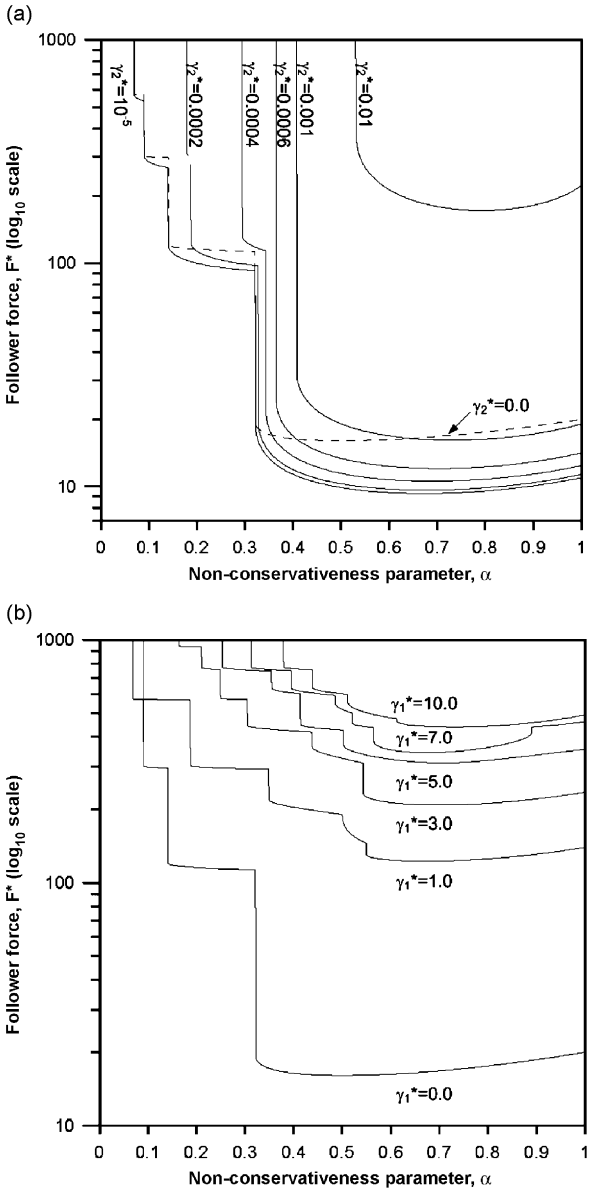

Fig. 19. Effect of internal and external damping on the instability region for the column with Winkler foundation. (a) $k_1^* = 10^5$ and $\gamma_1^* = 0.0$, (b) $k_1^* = 10^5$ and $\gamma_2^* = 0.0$.

Also, the divergence and flutter instability regions for a column subjected to partially tangential force are presented in Fig. 16 for various Winkler foundation parameters. When the Winkler foundation parameter is less than and greater than the critical value of the foundation parameter, the instability mechanism changes from divergence to flutter, and the critical load of the beam will jump upward and downward. According to the study by Lee et al. [59], the jump phenomenon occurs only at a single point. However, Fig. 16 shows more than one critical flutter-jumping points. In Fig. 16, the jump phenomena occur when the values of k_1^* are 41.45, 10671, 73500, and 267673, respectively, and their corresponding sub-tangentiality are 0.322, 0.141, 0.091, and 0.069, respectively. This can also be explained from the eigen-curves in Fig. 17. The instability mechanism changes from divergence to flutter by crossing over the turning point (point P in Fig. 16) and its corresponding value of k_1^* is 8526.7 when $\alpha = 0.2$. Fig. 17 shows that flutter occurs only when the third and fourth frequencies coalesce. Similarly, for $\alpha = 0.1$, $k_1^* = 10^5$, when the fifth and sixth frequencies coalesce, the flutter occurs, and the flutter load $F^* = 299$ is smaller than the first divergence load $F^* = 355.8$.

Fig. 18 shows the tip displacement as function of time and its frequency spectrum when $\alpha = 0.2$ and $k_1^* = 10^4$, where the critical flutter load is 115.62, so at a lower value than this flutter load, steady oscillation occurs and the first frequency governs the system. But as the load approaches to the critical point, the third and fourth frequencies coalesce and its magnitude of coalescent frequency is similar to that of the first frequency. Then as the load increases beyond the critical load as shown in Fig. 18(d), the coalescent frequency governs the system stability. Also the flutter-jump depends on the external and the internal damping. Fig. 19(a) shows the internal damping effect on the Beck's column with Winkler foundation. As shown in Fig. 19(a), the second and the third jump phenomena disappear when $0.0005 < \gamma_2^* < 0.0006$ and $0.0002 < \gamma_2^* < 0.0004$, respectively. The external damping effect is shown in Fig. 19(b). Fig. 19(b) shows that the external damping increases the critical flutter load of the column and the value of flutter-jumping point.

The influence of the Pasternak foundation on the instability region is depicted in Fig. 20. As the value of the Pasternak foundation parameter increases, the flutter load increases, as shown in Fig. 15, but the α corresponding to the occurrence of the flutter-jump decreases.

5. Conclusions

Using FE formulation based on the extended Hamilton's principle, the influences of the sub-tangentiality parameter, the external damping, the internal small damping, and the Winkler and Pasternak foundations on the dynamic stability of the Beck's column have been investigated. In addition, the effect of the growth rate of

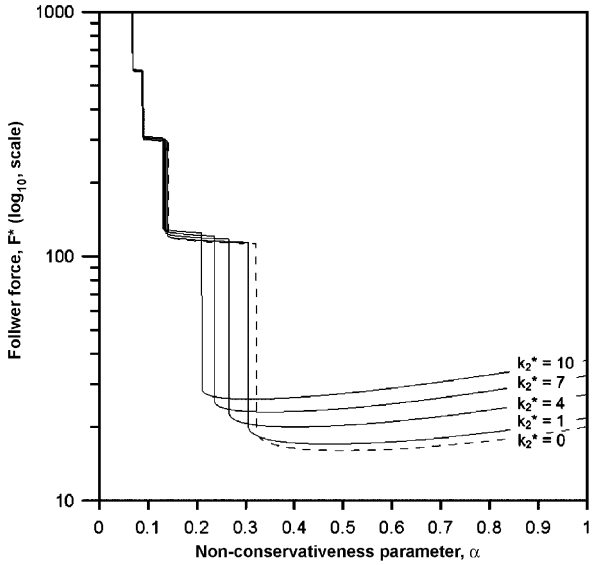

Fig. 20. Effect of Pasternak foundation on the instability region for the column, $k_1^* = 10^5$.

motion in a finite time interval and the effect of Winkler and Pasternak foundations on the non-conservative systems are reported. The distinction drawn from numerical example is summarized as follows:

1. The stability diagram for the Beck's column shows that the second flutter load is discontinuous at the transition point ($\alpha = 0.5$). Also the sub-tangentiality parameter α increases the first and the second flutter load.
2. Effects of the external and the internal damping on the non-conservative system may be effectively investigated by using the Rayleigh damping matrix. It is clear from the parametric study that the external damping compensates partly the destabilizing effect of internal damping.
3. Time history analysis shows that the real part of the fundamental complex frequency governs the dynamic stability behaviors of the non-conservative system. In the case of the column with small internal damping, it becomes positive and very small, which means weakly unstable.
4. Dynamic stability behaviors of the non-conservative system considering the external and the internal damping may be effectively traced by using concept of stability in a finite time interval.
5. The Pasternak foundation increases the flutter load as well as the divergence load of the column.
6. Particularly, the flutter-jump phenomena are observed depending upon the Winkler, Pasternak foundations, and the external, and the internal damping.

Acknowledgment

This work is a part of a research project supported by Korea Ministry of Construction & Transportation through Korea Bridge Design & Engineering Research Center at Seoul National University. The authors wish to express their gratitude for the financial support.

Appendix A. Detailed results of matrices $\mathbf{M_e}$, $\mathbf{K_e}$, $\mathbf{K_s}$, $\mathbf{K_g}$ and $\mathbf{K_{nc}}$

Mass matrix $\mathbf{M_e}$:

$$\mathbf{M_e} = \frac{\zeta}{420}\begin{bmatrix} 156 & 22\zeta & 54 & -13\zeta \\ & 4\zeta^2 & 13\zeta & -3\zeta^2 \\ & & 156 & -22\zeta \\ & \text{symm.} & & 4\zeta^2 \end{bmatrix}, \tag{A.1}$$

Elastic stiffness matrix $\mathbf{K_e}$:

$$\mathbf{K_e} = \frac{1}{\zeta^3}\begin{bmatrix} 12 & 6\zeta & -12 & 6\zeta \\ & 4\zeta^2 & -6\zeta & 2\zeta^2 \\ & & 12 & -6\zeta \\ & \text{symm.} & & 4\zeta^2 \end{bmatrix}. \tag{A.2}$$

Stiffness matrix considering the foundation effects $\mathbf{K_s}$:

$$\mathbf{K_s} = \frac{k_1^*\zeta}{420}\begin{bmatrix} 156 & 22\zeta & 54 & -13\zeta \\ & 4\zeta^2 & 13\zeta & -3\zeta^2 \\ & & 156 & -22\zeta \\ & \text{symm.} & & 4\zeta^2 \end{bmatrix} + \frac{k_2^*}{30\zeta}\begin{bmatrix} 36 & 3\zeta & -36 & 3\zeta \\ & 4\zeta^2 & -3\zeta & -\zeta^2 \\ & & 36 & -3\zeta \\ & \text{symm.} & & 4\zeta^2 \end{bmatrix}. \tag{A.3}$$

Geometric stiffness matrix due to an axial force $\mathbf{K_g}$:

$$\mathbf{K_g} = -\frac{F^*}{30\zeta}\begin{bmatrix} 36 & 3\zeta & -36 & 3\zeta \\ & 4\zeta^2 & -3\zeta & -\zeta^2 \\ & & 36 & -3\zeta \\ & \text{symm.} & & 4\zeta^2 \end{bmatrix}. \tag{A.4}$$

Load correction stiffness matrix $\mathbf{K_{nc}}$:

$$\mathbf{K_{nc}} = \alpha F^*\begin{bmatrix} \cdot & \cdot & \cdot & \cdot \\ \cdot & \cdot & \cdot & \cdot \\ \cdot & \cdot & \cdot & 1 \\ \cdot & \cdot & \cdot & \cdot \end{bmatrix}. \tag{A.5}$$

References

[1] H. Leipholz, *Stability of elastic systems*, Sijthoff and Noordhoff International Publishers BV, Alphen aan den Rijn, Netherlands, 1980.

[2] M.A. Langthjem, Y. Sugiyama, Dynamic stability of columns subjected to follower loads: a survey, *Journal of Sound and Vibration* 238 (2000) 809–851.

[3] W.T. Koiter, Unrealistic follower forces, *Journal of Sound and Vibration* 194 (1996) 636–638.

[4] Y. Sugiyama, M.A. Langthjem, B.-J. Ryu, Realistic follower forces, *Journal of Sound and Vibration* 225 (1999) 779–782.

[5] S.U. Ryu, Y. Sugiyama, Computational dynamics approach to the effect of damping on stability of a cantilevered column subjected to a follower force, *Computers and Structures* 81 (2003) 265–271.

[6] B.J. Ryu, Y. Sugiyama, Dynamic stability of cantilevered Timoshenko columns subjected to a rocket thrust, *Computers and Structures* 51 (1994) 331–335.

[7] Y. Sugiyama, K. Katayama, K. Kiriyama, Experimental verification of dynamic stability of vertical cantilevered columns subjected to a sub-tangential force, *Journal of Sound and Vibration* 236 (2000) 193–207.

[8] B.J. Ryu, K. Katayama, Y. Sugiyama, Dynamic stability of Timoshenko columns subjected to subtangential forces, *Computers and Structures* 68 (1998) 499–512.

[9] M.A. Langthjem, Y. Sugiyama, Optimum design of cantilevered columns under the combined action of conservative and nonconservative loads Part I: the undamped case, *Computers and Structures* 74 (2000) 385–398.

[10] M.A. Langthjem, Y. Sugiyama, Optimum design of cantilevered columns under the combined action of conservative and nonconservative loads Part II: the damped case, *Computers and Structures* 74 (2000) 399–408.

[11] R. Ishida, Y. Sugiyama, On the optimal shape of a column subjected to a follower force, *Transactions of the Japan Society of Mechanical Engineers* 63 (1997) 195–200.

[12] J.H. Kim, Y.S. Choo, Dynamic stability of a free–free Timoshenko beam subjected to a pulsating follower force, *Journal of Sound and Vibration* 216 (1998) 623–636.

[13] U.T. Ringertz, Optimization of eigenvalues in nonconservative systems, in: N. Olhoff, G.I.N. Rozvany (Eds.), *Proceedings of the First World Congress of Structural and Multidisciplinary Optimization*, 1995, pp. 741–748.

[14] M. Saje, G. Jelenic, Finite element formulation of hyperelastic plane frames subjected to nonconservative loads, *Computers and Structures* 50 (1994) 177–189.

[15] S. Del Giudice, G. Comini, C. Nonino, A physical interpretation of conservative and non-conservative finite element formulations of convection-type problems, *International Journal for Numerical Methods in Engineering* 35 (1992) 709–727.

[16] L.W. Chen, D.M. Ku, Stability analysis of a Timoshenko beam subjected to distributed follower forces using finite elements, *Computers and Structures* 41 (1991) 813–819.

[17] Y. Seguchi, M. Tanaka, S. Kojima, H. Takahashi, Shape determination of a cantilever column subjected to follower force, *Transactions of the Japan Society of Mechanical Engineers Series A* 55 (1989) 656–663.

[18] Y. Seguchi, Y. Tada, K. Kema, Shape decision of nonconservative structural systems by the inverse variable principle, *Transactions of the Japan Society of Mechanical Engineers Series A* 50 (1984) 679–686.

[19] R.S. Barsoum, Finite element method applied to the problem of stability of a nonconservative system, *International Journal for Numerical Methods in Engineering* 3 (1971) 63–87.

[20] G. Venkateswara Rao, R.V. Narasimha Rao, Galerkin finite element solution for the stability of cantilever columns subjected to a tangential loads, *AIAA Journal* 13 (1975) 690–691.

[21] I. Takahashi, Vibration and stability of a non-uniform cracked Timoshenko beam subjected to follower force, *Computers and Structures* 71 (1999) 585–591.

[22] I. Takahashi, Y. Yoshioka, Vibration and stability of a non-uniform double-beam subjected to follower forces, *Computers and Structures* 59 (1996) 1033–1038.
[23] S.Y. Lee, C.C. Yang, Non-conservative instability of non-uniform beams resting on an elastic foundation, *Journal of Sound and Vibration* 169 (1994) 433–444.
[24] T. Irie, G. Yamada, I. Takahashi, Vibration and stability of a non-uniform Timoshenko beam subjected to a follower force, *Journal of Sound and Vibration* 70 (1980) 503–512.
[25] H.P. Lee, Effects of damping on the dynamic stability of a rod with an intermediate spring support subjected to follower forces, *Computers and Structures* 60 (1996) 31–39.
[26] H.P. Lee, Dynamic stability of a tapered cantilever beam on an elastic foundation subjected to a follower force, *International Journal of Solids and Structures* 33 (1996) 1409–1424.
[27] H.P. Lee, Dynamic stability of a rod with an intermediate spring support subjected to subtangential follower forces, *Computer Methods in Applied Mechanics and Engineering* 125 (1995) 141–150.
[28] H.P. Lee, Divergence and flutter of a cantilever rod with an intermediate spring support, *International Journal of Solids and Structures* 32 (1995) 1371–1382.
[29] B. Nageswara Rao, G. Venkateswara Rao, Stability of a cantilever column under a tip-concentrated subtangential follower force with damping, *Journal of Sound and Vibration* 138 (1990) 341–344.
[30] B. Nageswara Rao, G. Venkateswara Rao, Stability of tapered cantilever columns subjected to a tip- concentrated follower force with or without damping, *Computers and Structures* 37 (1990) 333–342.
[31] B. Nageswara Rao, G. Venkateswara Rao, Stability of a cantilever column under a tip-concentrated subtangential follower force with the value of sub-tangential parameter close to or equal to 1/2, *Journal of Sound and Vibration* 121 (1988) 181–188.
[32] A. Guran, F.P.J. Rimrott, On the dynamic stability of an elastic rod under a slave tip loading., *In Vibration Analysis—Techniques and Applications, ASME, DE* 18 (1989) 225–228.
[33] S.Y. Lee, Y.H. Kuo, F.Y. Lin, Stability of a Timoshenko beam resting on a Winkler elastic foundation, *Journal of Sound and Vibration* 153 (1992) 193–202.
[34] M.A. De Rosa, C. Franciosi, The influence of an intermediate support on the stability behavior of cantilever beams subjected to follower forces, *Journal of Sound and Vibration* 137 (1990) 107–115.
[35] Y. Sugiyama, S.U. Ryu, M. Hamatani, T. Iwama, Computational approach to damped beck's column. *Physics and Control 2003, International Conference*, Vol. 4, 2003, pp. 1124–1129.
[36] Y. Sugiyama, K. Katayama, S. Knoi, Flutter of cantilevered column under rocket thrust, *Journal of Aerospace Engineering* 8 (1995) 9–15.
[37] C. Semler, H. Alighanbari, M.P. Païdoussis, A physical explanation of the destabilizing effect of damping, *Journal of Applied Mechanics* 65 (1998) 642–648.
[38] A.N. Kounadis, G.J. Smities, Local(classical) and global bifurcations in non-linear, non-gradient autonomous dissipative structural systems, *Journal of Sound and Vibration* 160 (1993) 417–432.
[39] A.N. Kounadis, *Non-gradient systems: the failure of static analyses in region of divergence stability and other phenomena*, Corso CISM, Udine, 1993.
[40] J.J. Thomsen, Chaotic dynamics of the partially follower-loaded elastic double-pendulum. Report No. 455, Technical University of Denmark, 1993.
[41] W.B. Krätzig, *Computational Concepts for Kinetic Instability Problems*, Corso CISM, Udine, 1993.
[42] W.B. Krätzig, L.Y. Li, P. Nawrotzki, Stability conditions for non-conservative dynamical systems, *Computational Mechanics* 8 (1991) 141–151.
[43] M.S. El Naschie, *Stress, Stability and Chaos in Structural Engineering. An Energy Approach*, MaGraw-Hill, New York, 1990.
[44] V.V. Bolotin, N.I. Zhinzher, Effects of damping on stability of elastic system subjected to non- conservative forces, *International Journal of Solids and Structures* 5 (1969) 965–989.
[45] V.V. Bolotin, *Nonconservative Problems of the Theory of Elastic Stability*, Pergamon, Oxford, 1963.
[46] V.V. Bolotin, *Dynamic Stability of Structures*, Corso CISM, Udine, 1993.
[47] H. Ziegler, Die stagilitätskriterien der Elastomechanik, *Ing Arch* 20 (1952) 49–56.
[48] T.E. Smith, G. Herrmann, Stability of a beam on elastic foundation subjected to a follower force, *Journal of Applied Mechanics, ASME* 39 (1972) 628–629.
[49] C. Sundararajan, Stability of column on elastic foundations subjected conservative and non-conservative forces, *Journal of Sound and Vibration* 37 (1974) 79–85.
[50] W. Hauger, K. Vetter, Influence of an elastic foundation on the stability of a tangentially loaded column, *Journal of Sound and Vibration* 47 (1976) 296–299.
[51] I. Elishakoff, X. Wang, Generalization of Smith–Hermann problem with the aid of computerized symbolic algebra, *Journal of Sound and Vibration* 117 (1987) 537–542.
[52] I. Elishakoff, A. Jacoby, Influence of various types of elastic foundation on the divergence and flutter loads of Zieglers model structure, *Journal of Applied Mathematics and Physics* 38 (1987) 779–784.
[53] G. Venkateswara Rao, K. Kanaka Raju, Stability of tapered cantilever columns with an elastic foundation subjected to a concentrated follower force at the free end, *Journal of Sound and Vibration* 81 (1982) 147–151.
[54] S.Y. Lee, Y.H. Kuo, F.Y. Lin, Stability of a Timoshenko beam resting on a Winkler elastic foundation, *Journal of Sound and Vibration* 153 (1992) 193–202.
[55] S.Y. Lee, C.C. Yang, Non-conservative instability of a Timoshenko beam resting on Winkler elastic foundation, *Journal of Sound and Vibration* 162 (1993) 177–184.

[56] *Microsoft IMSL Library* 1995, Microsoft Corporation.
[57] B.K. Lee, K.M. Choi, T.E. Lee, M.Y. Kim, Free vibration analysis of compressive tapered members resting on elastic foundation using differential quadrature method, *Journal of the Computational Structural Engineering* 15 (2002) 629–638.
[58] T. Yokoyama, Vibration analysis of Timoshenko beam-columns on two-parameter elastic foundation, *Computers and Structures* 61 (1996) 995–1007.
[59] S.Y. Lee, J.C. Lin, K.C. Hsu, Elastic instability of a beam resting on an elastic foundation subjected to a partially tangential force, *Computers and Structures* 59 (1996) 983–988.
[60] T.K. Caughey, M.E.J. O'Kelly, Classical normal modes in damped linear dynamic systems, *Journal of Applied Mechanics* 32 (1965) 583–588.